Materials Letters 62 (2008) 4220–4222

Contents lists available at ScienceDirect

Materials Letters

journal homepage: www.elsevier.com/locate/matlet

Enhancement of bifunctional catalysis by Ir doping of $La_{0.6}Ca_{0.4}CoO_3$ perovskites

Yun-Min Chang, Yu-Chi Hsieh, Pu-Wei Wu *, Chun-Han Lai, Tin-Yu Chang

Department of Materials Science and Engineering, National Chiao Tung University, Hsinchu 300, Taiwan, ROC

ARTICLE INFO

Article history:
Received 4 April 2008
Accepted 19 June 2008
Available online 22 June 2008

Keywords:
Perovskites
Catalysts
Bifunctional abilities
Alkaline electrolyte

ABSTRACT

$La_{0.6}Ca_{0.4}Co_{0.8}Ir_{0.2}O_3$ was prepared by solid state reaction synthesis from mixtures of $La(NO_3)_3{\cdot}6H_2O$, $Ca(NO_3)_2{\cdot}4H_2O$, $Co(NO_3)_3{\cdot}6H_2O$, and IrO_2 at stoichiometric ratio. Images from scanning electron microscopy on the as-synthesized powders exhibited particles in irregular shape at 100–250 nm in size. X-ray diffraction analysis confirmed the formation of perovskite without the rutile signals from IrO_2, suggesting successful incorporation of Ir^{4+} at the Co cation sites. The carbon nanocapsules (CNCs) were used as an electrocatalyst support. Electrodes for electrochemical measurements were fabricated by depositing mixtures of CNCs, $La_{0.6}Ca_{0.4}Co_{0.8}Ir_{0.2}O_3$, and polymeric binders on commercially available noncatalyzed gas diffusion electrodes. In alkaline electrolyte, the $La_{0.6}Ca_{0.4}Co_{0.8}Ir_{0.2}O_3$/CNCs demonstrated superior performances than those of $La_{0.6}Ca_{0.4}CoO_3$/CNCs and IrO_2/CNCs in both charging and discharging current–potential polarization measurements.

1. Introduction

Materials that promote both oxidation and reduction reactions on the same electrode are known as bifunctional electrocatalysts. In particular, considerable efforts have focused on identifying suitable electrocatalysts for the oxygen reduction and evolution because of potential applications in rechargeable metal–air and regenerative fuel cell [1,2]. To date, ceramics including perovskites (ABO_3), spinels (AB_2O_4), and dioxides (AO_2) have been evaluated for their electrochemical catalytic abilities [3]. Among them, the perovskites were studied extensively in various compositions. For example, the lanthanum cobaltate ($LaCoO_3$) is recognized for relatively simple synthesis and doping of various elements [4,5]. It was suggested by Tiwari et al. that the B site cations (i.e., Co^{3+}) in the $LaCoO_3$ are responsible for the observed catalytic behaviors in the oxygen reduction [6]. Therefore, the replacement of Co^{3+} with ones revealing better abilities is clearly a direction to pursue.

The iridium oxide (IrO_2) has been used as the dimensionally stable anode for chlor alkali cells [3]. The IrO_2 is known for superb electrical conductivities and corrosion resistances, attributes that are essential in many electrochemical reactions. Previously, De Pauli and Trasatti studied mixed oxides of IrO_2 and SnO_2, and reported impressive performances for the oxygen evolution in acid electrolyte [7]. With a rutile structure, the Ir^{4+} is surrounded by six neighboring oxygen anions forming an octahedron, much like the environment Co^{3+} experiences in the perovskite matrix. Therefore, there arises significant interest to synthesize perovskites with partial replacements of Ir^{4+} at the Co cation sites and characterize their bifunctional behaviors. Recently we synthesized a metastable $La_{0.6}Ca_{0.4}CoIr_{0.25}O_{3.5-\delta}$ and observed notable behaviors in both charging and discharging reactions [8]. However, the exact nature of the improvements was not clear because excess cations and anions were present in the perovskite lattice. In this work, we synthesized stoichiometric $La_{0.6}Ca_{0.4}Co_{0.8}Ir_{0.2}O_3$ by the solid state reaction route and evaluated its bifunctional catalytic abilities.

2. Experimental

In the solid state reaction synthesis, a mortar and pestle were used to grind and mix $La(NO_3)_3{\cdot}6H_2O$, $Ca(NO_3)_2{\cdot}4H_2O$, $Co(NO_3)_3{\cdot}6H_2O$, and IrO_2 at stoichiometric ratio (0.6:0.4:0.8:0.2). The mixtures were subjected to a two-stage calcination in air at 400 °C for 4 h and 800 °C for 4 h, respectively. The catalytic layer of the gas diffusion electrode (GDE) was fabricated by mixing 30 wt.% $La_{0.6}Ca_{0.4}Co_{0.8}Ir_{0.2}O_3$, 30 wt.% polytetrafluoroethylene (PTFE, Dupont T-30), 10 wt.% poly vinyl alcohol (PVA, Mw=2000–12,000), and 30 wt.% carbon nanocapsules (CNCs) in excess deionized water to make a slurry. After mixing for 3 min, the slurry was brush-painted repeatedly onto commercially available noncatalyzed GDEs (eVionyx Inc.) to reach a catalyst loading of 2.4 mg/cm^2. Afterwards, the GDEs were heated at 350 °C for 30 min to remove residual solvents. Lastly, the GDEs were rolled and pressed to reduce their thickness to 300 μm.

Electrochemical characterizations were conducted by a Solartron SI1287 potentiostat for analysis in current–potential (i–V) polarizations with a scan rate of 1 mV/s for both charging and discharging reactions. The electrolyte used was an aqueous solution containing 30 wt.% KOH. An area of 3 cm^2 on the backside of the GDE was exposed to ambient air during measurements. A Ti mesh coated with RuO_2/IrO_2 was used as the counter electrode and a Zn rod was selected as the

* Corresponding author. Tel.: +886 3 5131227; fax: +886 3 5724727.
E-mail address: ppwu@mail.nctu.edu.tw (P.-W. Wu).

0167-577X/$ – see front matter © 2008 Elsevier B.V. All rights reserved.
doi:10.1016/j.matlet.2008.06.040

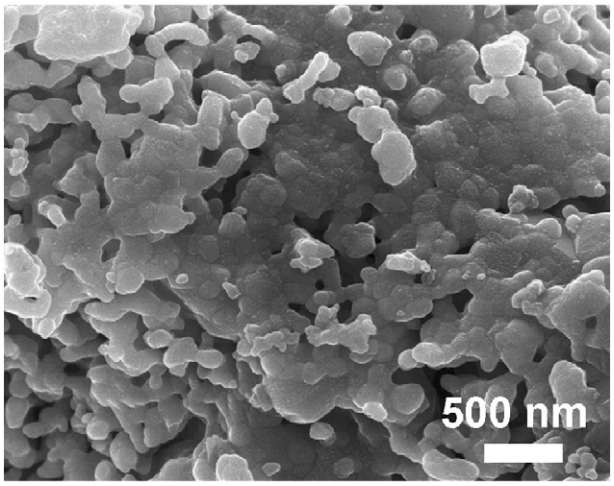

Fig. 1. The SEM image of $La_{0.6}Ca_{0.4}Co_{0.8}Ir_{0.2}O_3$ after the solid state reaction synthesis.

reference electrode. Thus the potential reading reflects the operation voltage of a zinc-air cell. In addition, the electrochemical measurements were carried out on the $La_{0.6}Ca_{0.4}CoO_3$ and IrO_2 serving as the reference. The $La_{0.6}Ca_{0.4}CoO_3$ was synthesized from the amorphous citrate precursor method (ACP) and its synthetic details were reported elsewhere [9]. Phase identification of the as-synthesized powders was conducted by a Siemens D5000 X-Ray Diffractometer with Cu K_α of 0.154 nm. The morphologies of the $La_{0.6}Ca_{0.4}Co_{0.8}Ir_{0.2}O_3$ particles were observed by a SEM (JEOL JSM-6700F). The values for surface area and density were obtained from TriStar 3000 (Micromeritics) and AccuPyc 1340 (Micromeritics), respectively.

3. Results and discussion

Fig. 1 provides the SEM image of the as-synthesized powders after the solid state reaction. The picture exhibited aggregates with substantial sintering and their primary particles were 100–250 nm in size. Fig. 2 presents the X-ray diffraction result of the as-synthesized powders along with the standard peaks of IrO_2 (JCPDS 15-0870) and $La_{0.6}Ca_{0.4}CoO_3$ (JCPDS 36-1389). Despite of minor signals labeled as Co_3O_4, the major

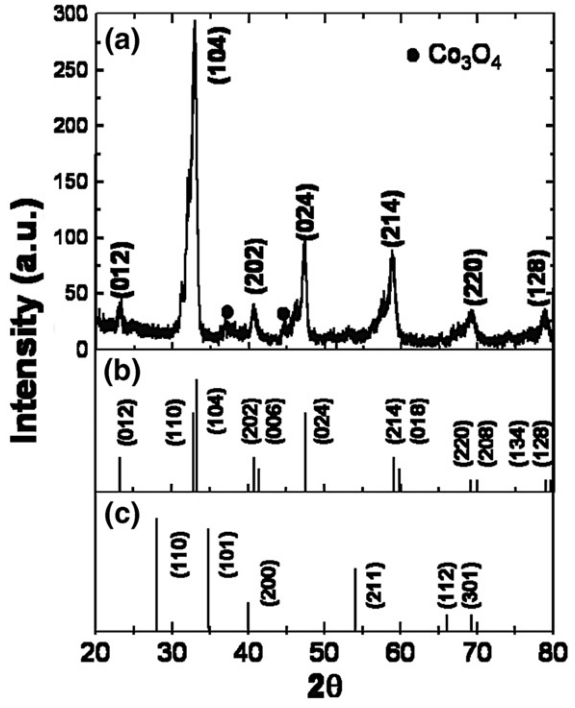

Fig. 2. The X-ray diffraction patterns of (a) the as-synthesized $La_{0.6}Ca_{0.4}Co_{0.8}Ir_{0.2}O_3$, (b) $La_{0.6}Ca_{0.4}CoO_3$ from JCPDS 36-1389, and (c) IrO_2 from JCPDS 15-0870.

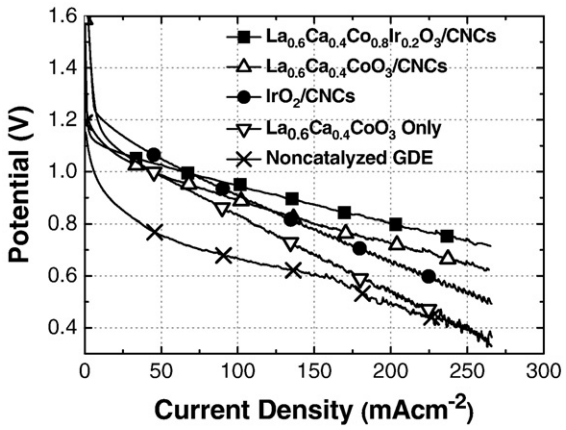

Fig. 3. The discharging *i–V* polarization curves of the noncatalyzed GDE, and catalyzed GDEs with electrocatalysts of $La_{0.6}Ca_{0.4}CoO_3$, IrO_2/CNCs, $La_{0.6}Ca_{0.4}CoO_3$/CNCs, as well as $La_{0.6}Ca_{0.4}Co_{0.8}Ir_{0.2}O_3$/CNCs.

diffraction peaks of the as-synthesized powders were consistent with those of hexagonal $La_{0.6}Ca_{0.4}CoO_3$. The signals from IrO_2 were notably absent. Calculation of the lattice parameters using high angle diffraction peaks arrives at 13.25 Å and 5.44 Å for *c* and *a* axis, respectively. These values are slightly larger than those of $La_{0.6}Ca_{0.4}CoO_3$ (c=13.09 Å and a=5.43 Å) from standard JCPDS. The volume expansion is not unexpected because the size of Ir^{4+} (0.76 Å) is larger than that of Co cation (Co^{3+}=0.69 Å and Co^{4+}=0.67 Å). In addition, the EDX mapping of the as-synthesized powders indicated uniform distributions of Ir. Our results suggest successful incorporation of Ir^{4+} at the Co cation sites, confirming the formation of $La_{0.6}Ca_{0.4}Co_{0.8}Ir_{0.2}O_3$. In addition, the values of density and surface area for the $La_{0.6}Ca_{0.4}Co_{0.8}Ir_{0.2}O_3$ powders were recorded at 5.73 g/cm^3 and 3.1 m^2/g. In contrast, the $La_{0.6}Ca_{0.4}CoO_3$ from the ACP route was measured at 5.54 g/cm^3 and 9.2 m^2/g, respectively.

Previously, we have identified the CNCs to be an excellent substrate for catalyst support [10,11]. The CNCs (330 m^2/g) were produced by incomplete combustion of C_2H_2 and O_2 with the resulting particles size between 10 and 30 nm. Detailed processing parameters for the CNCs fabrication were reported by Liu and Li [12]. Fig. 3 exhibits the *i–V* polarizations in discharging mode conducted on the GDEs that were catalyzed by $La_{0.6}Ca_{0.4}CoO_3$, IrO_2/CNCs, $La_{0.6}Ca_{0.4}CoO_3$/CNCs, and $La_{0.6}Ca_{0.4}Co_{0.8}Ir_{0.2}O_3$/CNCs. In addition, the noncatalyzed GDE was evaluated as the reference. In *i–V* profiles, the voltage readings started from 1.20 V and decreased gradually with increasing current. Among these discharging curves the $La_{0.6}Ca_{0.4}Co_{0.8}Ir_{0.2}O_3$/CNCs demonstrated the highest catalytic ability, delivering 0.948 V at 100 mA/cm^2. This is a significant 57 mV enhancement over that of $La_{0.6}Ca_{0.4}CoO_3$/CNCs. Interestingly, the $La_{0.6}Ca_{0.4}CoO_3$/CNCs behaved better than IrO_2/CNCs at high current density. In contrast, the unsupported $La_{0.6}Ca_{0.4}CoO_3$ showed rapid deteriorations in *i–V* measurement, approaching that of noncatalyzed GDEs at current density above 175 mA/cm^2. Synergistic effect of perovskites with carbonaceous materials was observed previously [13]. This behavior is expected because the carbon produces peroxide ions in the reduction reaction and presence of perovskites promotes decomposition of the peroxide ions.

The *i–V* polarizations in charging mode for the IrO_2/CNCs, $La_{0.6}Ca_{0.4}CoO_3$/CNCs, $La_{0.6}Ca_{0.4}Co_{0.8}Ir_{0.2}O_3$/CNCs, as well as noncatalyzed GDE are provided in Fig. 4. In charging reaction the oxygen was produced and released from the GDEs. Generally, the oxygen evolution exhibits a much severe polarization loss as compared to that of

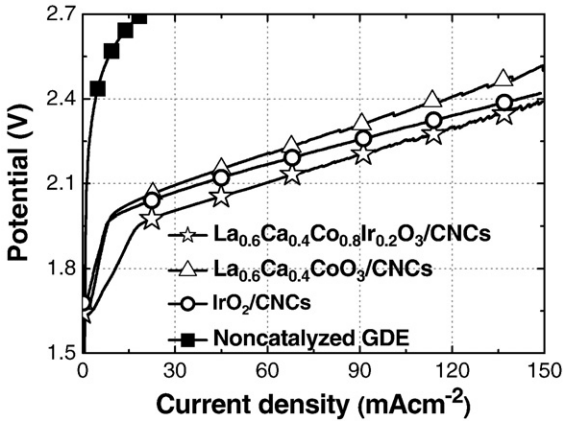

Fig. 4. The charging *i–V* polarization curves of the noncatalyzed GDE, and catalyzed GDEs with electrocatalysts of IrO_2/CNCs, $La_{0.6}Ca_{0.4}CoO_3$/CNCs, and $La_{0.6}Ca_{0.4}Co_{0.8}Ir_{0.2}O_3$/CNCs.

oxygen reduction at identical current density. From the diagram, the voltage started from 1.60 V and moved to higher values with increasing current density. The GDE catalyzed by $La_{0.6}Ca_{0.4}Co_{0.8}Ir_{0.2}O_3$/CNCs demonstrated impressive catalytic performances, showing a charging voltage of 2.39 V at 150 mA/cm^2. For current density between 0 and 150 mA/cm^2, the $La_{0.6}Ca_{0.4}Co_{0.8}Ir_{0.2}O_3$/CNCs exhibited a consistent performance improvement of 110 mV over that of $La_{0.6}Ca_{0.4}CoO_3$/CNCs. Although the IrO_2/CNCs was superior than that of $La_{0.6}Ca_{0.4}CoO_3$/CNCs, its performance was still inferior to that of $La_{0.6}Ca_{0.4}Co_{0.8}Ir_{0.2}O_3$. In contrast, the noncatalyzed GDE revealed negligible catalytic abilities with a sharp rise in the charging voltage. Our results confirmed the addition of Ir^{4+} in the lanthanum cobaltate is beneficial for bifunctional catalytic abilities. We would like to emphasize that in our measurements the surface area of $La_{0.6}Ca_{0.4}Co_{0.8}Ir_{0.2}O_3$ is smaller than that of $La_{0.6}Ca_{0.4}CoO_3$. Therefore, we are confident that the observed enhancements in *i*–*V* performances are due to the intrinsic superiority of $La_{0.6}Ca_{0.4}Co_{0.8}Ir_{0.2}O_3$.

4. Conclusions

Powders of $La_{0.6}Ca_{0.4}Co_{0.8}Ir_{0.2}O_3$ were synthesized by solid state reaction route. The SEM image revealed particles in irregular shape between 100 and 250 nm in size. Results from X-ray on the as-synthesized powders confirmed formation of perovskite phase with minor peaks of Co_3O_4. In electrochemical characterizations, the $La_{0.6}Ca_{0.4}Co_{0.8}Ir_{0.2}O_3$/CNCs exhibited improved performances over those of $La_{0.6}Ca_{0.4}CoO_3$/CNCs and IrO_2/CNCs for both charging and discharging polarizations in alkaline electrolyte.

Acknowledgements

The financial support from NSC (96-2221-E-009-110) is greatly appreciated. Carbon nanocapsules were provided by Professor Yuan-Yao Li of National Chung Cheng University.

References

[1] Shimizu Y, Uemura K, Matsuda H, Miura N, Yamazoe N. J Electrochem Soc 1990;137:3430–3.
[2] Jörissen L. J Power Sources 2006;155:23–32.
[3] Trasatti S. Transition metal oxides: versatile materials for electrocatalysis. In: Lipkowski J, Ross PN, editors. Electrochemistry of novel materials. New York: VCH Publishing Inc.; 1994. p. 207–95.
[4] Weidenkaff A, Ebbinghaus SG, Lippert T. Chem Mater 2002;14:1797–805.
[5] Wu NL, Liu WR, Su SJ. Electrochim Acta 2003;48:1567–71.
[6] Tiwari SK, Singh SP, Singh RN. J Electrochem Soc 1996;143:1505–10.
[7] De Pauli CP, Trasatti S. J Electroanal Chem 2002;538–539:145–51.
[8] Chang YM, Wu PW, Wu CY, Hsieh YF, Chen JY. Electrochem Solid-State Lett 2008;11:B47–50.
[9] Lee CK, Striebel KA, McLarnon FR, Cairns E. J Electrochem Soc 1997;144:3801–6.
[10] Wu CY, Wu PW, Lin P, Li YY, Lin YM. J Electrochem Soc 2007;154:B1059–1062.
[11] Lin YM, Chang YM, Wu PW, et al. J Appl Electrochem 2008;38:507–14.
[12] Liu TC, Li YY. Carbon 2006;44:2045–50.
[13] Kinoshita K. Electrochemical oxygen technology. New York: John Wiley & Sons; 1992.